blood

Prepublished online June 20, 2012;
doi:10.1182/blood-2012-01-406108

CD146 is a co-receptor for VEGFR-2 in tumor angiogenesis

Tianxia Jiang, Jie Zhuang, Hongxia Duan, Yongting Luo, Qiqun Zeng, Kelong Fan, Huiwen Yan, Di Lu, Zhongde Ye, Junfeng Hao, Jing Feng, Dongling Yang and Xiyun Yan

Blood (print ISSN 0006-4971, online ISSN 1528-0020), is published weekly by the American Society of Hematology, 2021 L St, NW, Suite 900, Washington DC 20036.

CD146 is a co-receptor for VEGFR-2 in tumor angiogenesis

Tianxia Jiang, Jie Zhuang, Hongxia Duan, Yongting Luo, Qiqun Zeng, Kelong Fan, Huiwen Yan, Di Lu, Zhongde Ye, Junfeng Hao, Jing Feng, Dongling Yang, Xiyun Yan*

Key Laboratory of Protein and Peptide Pharmaceutical, National Laboratory of Biomacromolecules, Chinese Academy of Sciences-University of Tokyo Joint Laboratory of Structural Virology and Immunology, Institute of Biophysics, Chinese Academy of Sciences, 15 Datun Road, Beijing 100101, China.

*Correspondence author: Xiyun Yan, Institute of Biophysics, Chinese Academy of Sciences, 15 Datun Road, Beijing 100101, China.

Email: yanxy@ibp.ac.cn

Tel.: +86 10 64888583. Fax: +86 10 64888584.

Short title: CD146 is a co-receptor for VEGFR-2

CD146 is a novel endothelial biomarker and plays an essential role in angiogenesis. However, its role in the molecular mechanism underlying angiogenesis still remains poorly understood. Here, we show that CD146 directly interacts with VEGFR-2 on endothelial cells as well as at the molecular level. The detail structural basis of CD146 binding to VEGFR-2 is identified. In addition, we show that CD146 is required in VEGF-induced VEGFR-2 phosphorylation, AKT/p38 MAPKs/NF-κB activation and thus promotion of endothelial cell migration as well as microvascular formation. Furthermore, anti-CD146 AA98 or CD146 siRNA abrogated all VEGFR-2 activation induced by VEGF. An *in vivo* angiogenesis assay showed that VEGF-promoted microvascular formation was impaired in the endothelial conditional knockout of CD146 ($CD146^{EC\text{-}KO}$). Importantly, our animal experiments demonstrated that anti-CD146 (AA98) and anti-VEGF (Bevacizumab) play an additive inhibitory effect on xenografted human pancreatic and melanoma tumor. Our findings suggest that CD146 is a new co-receptor for VEGFR-2 and a promising target for blocking tumor-related angiogenesis.

Introduction

Angiogenesis, the formation of new capillaries from pre-existing microvasculature, is a complex and crucial process during embryogenesis, female reproductive cycle, chronic inflammatory disorders, and tumor growth.[1] Many tumor masses secrete several kinds of angiogenic factors , such as vascular endothelial growth factor (VEGF), transforming growth factor-α (TGFα), and tumor necrosis factor (TNF) to promote blood vessel formation which eventually functions as a route for tumor metastasis.[2]

Among these angiogenic factors, VEGF is the most prominent one, whose family includes VEGF-A, VEGF-B, VEGF-C, VEGF-D, VEGF-E and placental growth factor (PIGF). They bind to three associated transmembrane tyrosine kinase receptors, known as VEGFR-1(Flt-1), VEGFR-2 (KDR or FIk-1) and VEGFR-3(FIt-3). VEGFR-2 is a key receptor for the development of the blood vasculature,[3] while VEGFR-3 is mainly involved in lymphogenesis.[4] Hence, targeting the VEGF-A/VEGFR-2 pathway has become an attractive strategy for anti-angiogenesis and tumor therapy.[2, 5] For instance bevacizumab, a very popular anti-VEGF-A antibody, has been used for the treatment of several cancers.[6-9] However, it was recently reported that some patients are intrinsically refractory or acquired resistant to bevacizumab.[10] Thus development of new or adjunct therapies would be of great benefit to patients.

CD146 is a cell adhesion molecule belonging to the immunoglobulin superfamily. It was originally considered as a melanoma marker promoting melanoma growth and metastasis.[11] Recently, increasing evidence suggests that CD146 is an endothelial biomarker and promotes angiogenesis.[12, 13] CD146 knockdown impaired cardiovascular development and blocked tumor angiogenesis in zebrafish.[14] Our previous work showed that an anti-CD146 antibody, named as AA98, inhibited endothelial cell migration and angiogenesis and human tumor growth in xenografted tumor mice.[15] In

addition, we found that CD146 plays an important role in cell migration that is specifically detected in invasive intermediate trophoblasts but not in non-invasive and in pre-eclampsia.[16, 17] Recently, we reported that CD146 is an epithelial-mesenchymal transition inducer and promotes the invasion of triple-negative breast cancer.[18]

Although CD146 has been considered as a receptor in endothelial cells, its ligand is still unknown.[19] Our previous studies showed that tumor secretion induced CD146 dimerization, p38 MAPKs/NF-κB activation and the up-regulation of many angiogenic genes including VEGF, MMP-9 and IL-8, and that anti-CD146 mAb (AA98) interfered with this CD146-mediated signaling.[20,21] In addition, Anfosso *et al.* found that CD146 associated with tyrosine kinase $p59^{Fyn}$ to phosphorylate $p125^{Fak}$ and paxillin, thus promoting endothelial cell migration.[22,23] However, the molecular mechanism of how CD146 functions as a receptor in angiogenesis still remains poorly understood.

Here we show for the first time that CD146 interacts with VEGFR-2 in the endothelium, and subsequently promotes angiogenesis *in vitro* and *in vivo*. Moreover, this CD146 and VEGFR-2 interaction and its mediated signal transduction could be blocked by anti-CD146 mAb AA98 or CD146 siRNA. Most importantly, our animal experiments demonstrated that a combinatorial therapy with anti-CD146 AA98 and anti-VEGF (bevacizumab) has an additive killing effect on both human pancreatic carcinoma and human melanoma. Our findings not only reveal the mechanism of how CD146 plays an important role in angiogenesis, but also provide a novel insight for combinatorial therapy of tumor angiogenesis.

Methods

Cells and animals

Human pancreatic carcinoma SW1990 cells and the human melanoma A375 cells were obtained from the American Type Culture Collection (Rockville, MD, USA). Human umbilical vein endothelial cells (HUVECs) were purchased from CellSystems (Biotechnologie Vertrieb GmbH, Katharinen, Germany). For the generation of CD146-expressing stable human embryonic kidney cell line HEK293T clones, HEK293T cells were transfected with human PBudCE4.1-CD146 using the Fugene HD method (Roche, indianapolis, IN, USA) and selected using zeocin (500 μg/ml). HEK293T cells stably transfected with CD146 were cultured in Dulbecco's modified Eagle's medium (Gibco Life Technologies Inc., Paisley, UK) with 1 g/L glucose, 10% fetal calf serum, 100 U/ml penicillin, and 100 μg/ml streptomycin. All cells were grown at 37°C and 5% CO_2.

All animal experiments were performed in compliance with the guidelines for the care and use of laboratory animals and were approved by the Biomedical Research Ethics Committee of the Institute of Biophysics, Chinese Academy of Sciences. BALB/c nude mice were obtained from the Animal Center of the Chinese Academy of Medical Science, Beijing. $Tek^{cre/+}CD146^{floxed/floxed}$ mice were generated using a Cre/loxP recombination system. $Tek^{+/+}CD146^{floxed/floxed}$ mice were backcrossed to a C57BL/6J background for a minimum of nine generations for obtaining $Tek^{cre/+}CD146^{floxed/floxed}$ mice (named $CD146^{EC\text{-}KO}$). $Tek^{+/+}CD146^{floxed/floxed}$ (named WT) mice were used as controls in Matrigel plugs assays. Genotyping of each generation was carried out using PCR. The complete absence of CD146 from the endothelial cells of vascular vessels was confirmed using immunohistochemistry and immunofluorescence.

Antibodies and reagents

Mouse anti-human CD146 mAbs, AA98[12] and AA1[24], were made in our

laboratory. Bevacizumab was from Roche (Indianapolis, IN, USA). Goat-anti-rabbit Alexa Flour 555 and goat-anti-rat-488 were from Invitrogen (San Diego, CA, USA). Mouse IgG (mIgG), human IgG (hIgG), FLAG (clone M2) were from Sigma-Aldrich (St. Louis, MO, USA). Antibodies against human NF-κB p50 and IκBα were from Santa Cruz Biotechnology (Santa Cruz, CA). Antibodies specific for Flk-1, phosphor-p38 MAPK, p38 MAPK, phospho-NF-κB p65 (Ser536), phospho-Erk, p44/42MAPK and phospho-p44/42 MAPK (T202/Y204) were from Cell Signaling Technology (Cell Signaling, Danvers, MA, USA). Antibodies against phospho-VEGFR-2 (Tyr 1214), phospho-AKT (Ser 473) were from Signalway Antibody (Pearland, TX, USA). HRP-conjugated goat anti-mouse or rabbit IgG were from GE Healthcare (Piscataway, NJ, USA). Antibody specific for CD31 was from Abcam (Cambridge, MA, USA). Rat anti-human CD146 (clone ME-9F1) was from BD Biosciences (Franklin Lakes, NJ, USA). Biotin-conjugated secondary antibodies, HRP-conjugated streptavidin were from Dianova (Rodeo, CA). DAPI was from Roche (Indianapolis, IN, USA).

Human recombinant VEGF-A165 was obtained from Upstate Biotechnology. Goat serum and DAB substrate system were from Santa Cruz Biotechnology (Santa Cruz, CA). Enhanced chemiluminescence assay kits were from Pierce (Rockford, IL, USA). Growth factor-reduced Matrigel was from BD Biosciences (Franklin Lakes, NJ, USA).

Constructs and transfection

The pCDNA3.1-(b)-CD146, pCDNA3.1-(b)-CD146/C452A, and Flag-CD146-$^{\triangle}$KKGK has been described previously.[21,25] The moesin construct lacking the actin-binding domain (MSN-$^{\triangle}$ABD) was generated by a polymerase chain reaction-based approach using Flag-MSN as a template. Fugene HD mediated transfection was employed according to the manufacture's instruction.

RNA interference

Double-stranded RNAs (dsRNA) targeting CDS: 410–428 of CD146 and the CDS: 1562–1580 of GFP, respectively, were synthesized by Invitrogen using sequences as previously described.[21]

For siRNA transfections, HUVECs were transfected with 50 nM of either GFP siRNA or CD146 siRNA, using the Fugene HD method. Cells were then incubated for 36 h at 37°C and 5% CO_2.

In vitro pull-down assays

0.15 μg Fc or Fc-sVEGFR-2 was conjugated to protein G agarose beads (Santa Cruz Biotechnology, Santa Cruz, CA). The beads were then incubated with 0.15 μg His-sCD146 protein for 1 h at 4°C. Proteins bound to the beads were then boiled in sample loading buffer and subjected to immunoblotting analysis.

Co-immunoprecipitation

HUVECs were lysed in a culture dish by adding 0.5 ml ice-cold RIPA lysis buffer for 30 min. The supernatants were collected by centrifugation at 12,000 g for 10 min at 4°C and then precleared with protein G-Sepharose to remove the protein G-bound proteins. The cleared lysates were then incubated with antibodies at 4°C overnight, followed by incubation with protein G-Sepharose for 4 h. Immunoprecipitates were washed three times with lysis buffer and then boiled for 5 min in loading buffer.

Activation of RTKs and downstream signals

Serum-starved HUVECs (24 h) were incubated with blocking reagents (50 μg/ml mAbs AA98 or AA1) or transfected with siRNA (CD146-siRNA or GFP-siRNA) prior to induction with VEGF-A165 (50 ng/ml) at 37°C for 10 min, 30 min, or 12 h for analysis of the activation of VEGFR-2, p38/AKT/Erk, and NF-κB, respectively. Cells were washed with ice-cold PBS, lysed in RIPA lysis buffer and then subjected to Western blotting as described. Blots were probed separately with anti-phosphorylated antibodies against VEGFR-2, Erk, p38,

and AKT, then stripped (62.5 mM Tris pH 6.8, 2% SDS, 0.8% DTT) and re-probed with their corresponding specific antibodies as loading control.

Immunofluorescence

Cells were plated on slides cultured in six-well plates and then subjected to appropriate treatments. After stimulation for 24 h with VEGF-A165 (50 ng/ml), the cells were washed with PBS, fixed in acetone:methanol (1:1) for 30 s, permeabilized with 0.1% Triton X-100, blocked with 5% normal goat serum for 60 min at 37°C, and then incubated with anti-p65 or anti-p50 for I h. Coverslips were subsequently examined with a confocal laser scanning microscope (Olympus, Tokyo, Japan).

Tube formation

The tube formation assay was performed as described by Nagata et al.[26] Tube formation was observed under an inverted microscope (Eclipse Model TS100; Nikon, Japan). Images were captured with a CCD color camera (Model KP-D20AU; Hitachi, Japan) attached to the microscope and tube length was measured using NIH ImageJ software.

Cell migration assay

Cell migration was assayed using a modified Boyden chamber assay as described (8-μm pore size; Costar, Corning, NY).[27] After the appropriate treatments, cells were trypsinized, washed, and resuspended in fresh serum-free medium (10,000 cells per well). After incubation at 37°C overnight, cells remaining at the upper surface of the membrane were removed using a swab, while cells that migrated to the lower membrane surface, representation of migrated cells, were fixed with 4% PFA and stained with Giemsa solution. The number of cells migrating through the filter was counted and plotted as the number of migrating cells per optic field (20X).

Immunohistochemistry

For 3,3'-Diaminobenzidine (DAB) staining, paraffin-embedded tissue sections were deparaffinized and stained first with an antibody specific for CD31, and then with biotin-conjugated secondary antibodies (1:1000), followed by HRP-conjugated streptavidin (Dianova, Rodeo, CA). The sections were finally counterstained with hematoxylin. The number of blood vessel per tumor in each group was quantified in at least 10 random areas per section. Images were taken using an inverted microscope (Eclipse Model TS100; Nikon, Japan).

For immunohistofluorescence, sections 5 μm in thickness were deparaffinized and stained with antibodies specific for CD31 and CD146, followed by fluorescent-labeled secondary antibodies. Nuclei were stained with DAPI.

***In vivo* angiogenesis assay**

Age- and sex-matched $CD146^{EC\text{-}KO}$ mice and wild-type mice were used. Mice were injected with 200 μl of growth factor-reduced Matrigel containing 60 units/ml of heparin (Sigma-Aldrich, St. Louis, MO, USA), mixed with VEGF-A165 (20 ng/ml) and sacrificed 7 days after implantation. The Matrigel plugs were dissected out immediately and blood-vessel infiltration was quantified by analyzing CD31-stained parafirm sections (as above).

Animal experiment

Female 4-week-old BALB/c nude mice were used and kept under specific pathogen-free conditions. Xenografts of human tumor cell lines were produced by injecting tumor cells ($1X10^7$ resuspended in PBS) subcutaneously into the back of the mice. When tumors reached a diameter of 3 to 5 mm, the mice were grouped (10 mice per group) and administered intraperitoneally with purified mAb AA98, AA1, human IgG, mIgG, bevacizumab alone, or bevacizumab plus AA98, at a dose of 200 μg per mouse, twice per week. Tumor size was measured twice per week and tumor volume was determined according to the following equation: tumor size = $width^2$ X length X (1/2).

Statistical analysis

All experiments were done in triplicate. Data are shown as means±SEM. Statistical differences were determined by unpaired Student's *t* tests. The statistical differences of "*in vivo* Matrigel Plug Assay" were determined by paired Student's *t* tests. A *p* value of 0.05 was considered significant.

Results

CD146 interacts with VEGFR-2 in endothelial cells

The co-expression of CD146 and VEGFR-2 on endothelial cells and the finding that tumor secretions containing VEGF and FGF induced CD146-mediated p38 MAPKs/NF-κB signaling led us to hypothesize that CD146 may act as a co-receptor for VEGFR-2. To test this, we performed co-immunoprecipitation (Co-IP) experiments to detect the interaction of CD146 and VEGFR-2 in two cell lines, human umbilical vein endothelial cells (HUVECs) with endogenous CD146 and VEGFR-2, and VEGFR-2 transfected HEK293T cells. As shown in Figure 1A, in HUVECs, VEGFR-2 was immunoprecipitated by anti-CD146 antibody and CD146 was immunoprecipitated by anti-VEGFR-2 antibody. This result was confirmed in VEGFR-2 transfected HEK293T, showing that CD146 was coimmunoprecipitated by anti-VEGFR-2 antibody in HEK293T cells co-expressing VEGFR-2 and CD146, but not from the cells expressing CD146 alone (Figure 1B). In addition, we also found that CD146 did not interact with VEGFR-1 (Figure S7).

To further investigate whether or not CD146 directly interacts with VEGFR-2, we carried out *in vitro* pull down assays using soluble CD146 (His-tagged CD146 extracellular domain, His-sCD146) and soluble VEGFR-2 (Fc-tagged VEGFR-2 extracellular domain, Fc-sVEGFR-2). Results showed that Fc-sVEGFR-2 was specifically bound to His-tagged CD146 as it bound to VEGF. In contrast, neither Fc nor Fc-beads were bound by His-sCD146 (Figure 1C). These data demonstrate a direct interaction between the CD146 extracellular domain and VEGFR-2.

Next, we ascertained whether the interaction of CD146 and VEGFR-2 could be abrogated by anti-CD146 antibody. To test a possible structural basis of CD146 binding to VEGFR-2, we used two different anti-CD146 antibodies, AA98 and AA1. AA98 recognizes a conformational epitope at C452–C499,

whereas AA1 recognizes a linear epitope at aa50–54 in the N-terminal domain.[21] Figure 1D showed that the interaction between CD146 and VEGFR-2 was markedly blocked by AA98 but not by AA1. To confirm this observation, we performed the Co-IP experiment in HUVECs using CD146/C452A mutant and found that the endogenous interaction of CD146 and VEGFR-2 was abrogated by the CD146/C452A mutation (Figure 1E), suggesting that C452 in domain five of CD146 contributes to the interaction of CD146 and VEGFR-2. This may explain why the anti-CD146 antibody, AA98 but not AA1 inhibited this interaction.

CD146 enhances VEGFR-2 phosphorylation and downstream signaling

As CD146 associated with VEGFR-2, we next asked whether CD146 transduces VEGF-activation signals. For this purpose, we used VEGF as a stimulator, and anti-CD146 AA98 and CD146 siRNA as inhibitors to evaluate the function of CD146 on VEGF-induced signaling pathway. As shown in Figure 2, we found that VEGF could induce VEGFR-2 phosphorylation, p38/IKK/NF-κB signaling cascade and Akt signal transduction. However, the VEGF-induced downstream signals were completely abrogated by the anti-CD146 mAb AA98 but not affected by AA1 (Figure 2A-E). Immunofluorescent staining of NF-κB p65 and p50 also confirmed that the nuclear translocation induced by VEGF was suppressed by AA98 treatment, but not by the control antibody, AA1 (Figure 2F). Consistent with these results, HUVECs transfected with a CD146/C452A mutant also inhibited VEGF-activated VEGFR-2 phosphorylation and downstream signal transduction (Figure S1).

We next analyzed the effect of CD146 siRNA on the activation of signals downstream of VEGFR-2. Results showed that the VEGF-activated VEGFR-2 phosphorylation, p38/IKK/NF-κB signaling cascade and Akt signaling were impaired by CD146 knockdown and rescued after restoring CD146 (Figure

3A-D). In addition, nuclear translocation of NF-κB p65 and p50 induced by VEGF was also inhibited by CD146-siRNA and re-activated by restoring CD146 expression (Figure 3E). In contrast, VEGF-induced Erk signaling was not affected by either AA98 or CD146-siRNA (Figure S2), implying that CD146 was mainly involved in the VEGF-induced Akt and p38/IKK/NF-κB pathways.

To test whether CD146 function is specifically dependent on VEGF, we repeated the experiments with TNFα, another angiogenic factor. We found that neither AA98 nor CD146 siRNA had any effects on the response of NF-κB to TNFα stimulation (Figure S3), suggesting that the response of CD146 to VEGF is specific.

Taken together, these data strongly suggest that CD146, as a VEGFR-2 co-receptor, is involved in regulating VEGF-induced VEGFR-2 downstream signals.

CD146 mediated ERM recruitment is essential for VEGF-mediated signal transduction and cell migration

We previously reported that CD146 interacted physically with ERM proteins (Ezrin-Radixin-Moesin) leading to the subsequent promotion of cell migration. The conserved positively-charged amino-acid cluster KKGK motif is responsible for the interaction of CD146 and ERM in this process.[25] It has been shown that some co-receptors such as CD44, interacts with ERM proteins and the cytoskeleton to promote signaling efficiently. CD44v6, VEGFR-2/c-Met, ERMs and the cytoskeleton form a signalosome.[25,28] To evaluate whether this mechanism is also essential for VEGFR-2 signaling, we transfected HUVECs with a CD146 construct lacking the KKGK motif (CD146-$^{\triangle}$KKGK) or a moesin construct lacking the actin-binding domain (MSN-$^{\triangle}$ABD).

As shown in Figure 4A-B, we found that either CD146-$^{\triangle}$KKGK or MSN-$^{\triangle}$ABD disturbed VEGF-induced VEGFR-2 downstream signaling without affecting

VEGFR-2 phosphorylation. In addition, HUVECs transfected with CD146-△KKGK or MSN-△ABD showed loss of migration capability (Figure 4C-D). These data suggest that the interaction of CD146 and ERM is essential for VEGF-induced signal transduction and cell migration.

CD146 is required in cell migration and tube formation induced by VEGF

To investigate the function of CD146 in the VEGF-promoted angiogenesis process, we performed endothelial cell migration and tube formation assays in the presence of AA98 and AA1. First, we tested the role of CD146 in VEGF-induced endothelial cell migration. As shown in Figure 5A, VEGF-induced motility of HUVECs was strongly suppressed by AA98, but not by AA1.

In addition, VEGF-stimulated cell migration was significantly impaired after CD146 knockdown in HUVECs, and rescued after transfection with a CD146-expressing construct. Quantification of the number of migrated cells revealed a 1.5-fold increase in VEGF-stimulate HUVEC migration which was abrogated by CD146-siRNA treatment (Figure 5C).

Next, we examined the function of CD146 on *in vitro* angiogenesis induced by VEGF. A tube formation assay was performed by growing endothelial cells in matrigel with either anti-CD146 antibody AA98 or AA1. Results showed that VEGF promoted endothelial tubular morphogenesis and accelerated tube formation. However, in the presence of AA98, the length of vessels decreased by 50% compared with that in the presence of AA1 (Figure 5B). This VEGF-promoted tube formation was also found to be markedly suppressed when CD146 was knocked-down in HUVECs by transfecting with CD146-siRNA. Tubular morphogenesis could be rescued by restoring CD146 levels (Figure 5D).

Moreover, we found that the CD146 mediated-tube formation is specifically dependent on VEGF, because when TNFα was used as a stimulator, neither CD146 knockdown nor anti-CD146 AA98 affected the angiogenic process (Figure S4). This may also help explain the more profound effect of AA98 on angiogenesis in vitro than *in vivo*.

VEGF-induced angiogenesis is impaired in CD146^{EC-KO} mice

To explore the potential role of CD146 in VEGF-mediated angiogenesis *in vivo*, we used a matrigel plug model in which matrigel mixed with VEGF is injected subcutaneously into age-and sex-matched CD146^{EC-KO} and wild type mice. In this system, endothelial cells migrate into the matrigel and form a capillary network. One week post-implantation, the numbers of blood vessels are counted by immunofluorescence using the blood vessel marker, CD31. Our results showed that the microvascular density of the matrigel plugs in CD146^{EC-KO} mice decreased to 47% when compared to that of the wild-type mice and no large vascular tubes were seen (Figure 6), indicating that the VEGF-induced angiogenic response is dependent on CD146 *in vivo*.

AA98 and Bevacizumab cumulatively inhibit human pancreatic carcinoma growth

It has been well documented that tumor growth is dependent on angiogenesis, and both AA98 and bevacizumab have previously been reported to inhibit tumor angiogenesis.[12,29,30] Our finding that CD146 acts as a co-receptor for VEGFR-2 prompted us to determine whether AA98 and bevacizumab could produce an additive effect on inhibiting tumor growth. We developed a tumor model using the human pancreatic carcinoma cells, SW1990, that express neither CD146 nor VEGFR-2 (Figure S5). Thus neither AA98 nor bevacizumab

could target the actual tumor cells and therefore any reduction in tumor growth would be the result of an anti-angiogenic effect. Antibody treatment was started when tumors reached a diameter of 5 to 6 mm. Our results showed that the growth of the human pancreatic carcinoma was markedly suppressed by treatment with AA98, bevacizumab and AA98+bevacizumab. A significant reduction in the tumor volume and weight was seen in AA98 or bevacizumab-treated groups when compared with the control groups treated with mIgG, hIgG and AA1 suggesting a role for CD146 and VEGF in the pancreatic carcinoma growth. It is interesting that the combinatorial treatment with AA98 and bevacizumab shows a significant inhibitory effect on the growth of the pancreatic tumor (70%), which is more efficient than AA98 (46%) and bevacizumab (48%) alone (Figure 7A-C; $p<0.001$, AA98+ bevacizumab versus AA98; $p<0.001$, AA98+bevacizumab versus bevacizumab) suggesting that the two agents act, at least in part, on different pathways.

In immunohistochemical analysis of the treated tumors, we observed a significant reduction of microvessel density in both AA98 and bevacizumab treated groups. However, in the AA98+bevacizumab combination treated group, the vessel numbers were approximately 40% and 30% less than that of AA98 or bevacizumab treatment alone (Figure 7D).

In addition, we also found this additive effect of AA98 and bevacizumab on another tumor model: human melanoma xenografted mice with A375 cells (Figure S6).

These data suggest that the combination of AA98 with bevacizumab to target tumor angiogenesis could eventually be used in a clinical setting.

Discussion

There is increasing evidence supporting a role for CD146 in angiogenesis.[12,15] We hypothesized that a possible link between CD146 and VEGFR-2 existed as both are endothelial markers and involved in Akt and p38 MAPK downstream signaling to promote endothelial cell migration and angiogenesis. However, there has been no direct evidence demonstrating the relationship between CD146 and VEGFR-2. In this study, we show for the first time that CD146 directly interacts with VEGFR-2 in endothelial cells and functions as a co-receptor for VEGFR-2 to enhance VEGF-induced signal transduction and angiogenesis. Several lines of evidence support the role of CD146 as a co-receptor for VEGFR-2. Firstly, the interaction of CD146 and VEGFR-2 was detected not only on endothelial cells that endogenously express both molecules, but also existed in VEGFR-2 transfected HEK293T as well as between the two soluble molecules. The structural basis for this interaction is located in the extracellular domain around aa452 of CD146 because the CD146/C452A mutant and anti-CD146 (AA98) targeting to C452-C499 could block this interaction. However, a different anti-CD146 (AA1) targeting aa50-54 did not affect the CD146-VEGFR-2 interaction. Secondly, CD146 enhanced VEGF-induced VEGFR-2 phosphorylation as well as downstream signaling, which leads to cell migration and blood vessel formation. Furthermore, VEGF-induced AKT/p38 MAPK/NF-κB signals could be abolished by the CD146 specific antibody AA98 and CD146 siRNA. In addition, our *in vivo* angiogenesis assay showed that vascularization is significantly impaired in $CD146^{EC\text{-}KO}$ mice. Lastly, the combination of anti-CD146 AA98 and anti-VEGF bevacizumab showed an additive function in the treatment of human pancreatic carcinoma and melanoma in xenografted mice.

Although several VEGFR-2 co-receptors,[31-35] including Neuropilin-1,[36]

Neuropilin-2[37] and CD44v6,[28] have been reported to play a role in VEGFR-2 signaling and angiogenesis, we found that unlike Neuropilin-1 and Neuropilin-2, whose interactions with VEGFR-2 are dependent on VEGF treatment, and mainly involved in the VEGFR-2-Erk pathway which eventually results in cell proliferation, the interaction of CD146 with VEGFR-2 is independent of VEGF treatment (data not shown), and is involved in the VEGF-mediated p38 MAPKs and AKT signaling pathway which culminates in cell migration. These observations suggest that the different VEGFR-2 co-receptors may trigger different downstream signals resulting in different cell functions. Thus, it is of particular interest to elucidate the relationship of these co-receptors, such as CD146, CD44v6 or Neuropilin-2, in VEGF-mediated angiogenesis.

There also exists common mechanism for VEGFR-2 co-receptors signaling. Both the cytoplasmic tail of CD146 and CD44 recruits ERM proteins and cytoskeleton for VEGF-induced signal transduction, suggesting that a scaffold is necessary for linking the intracellular signaling molecules together at the docking site of VEGFR-2. In addition, as is the case for PDGFRs, which have no known co-receptor, ERMs are needed for signal transduction.[38] Binding of ERM proteins to the cytoskeleton may thus be a common mechanism essential for signal transduction.

Based on all the above observations, we conclude that the regulation of CD146 as a VEGFR-2 co-receptor in the VEGF signaling pathway and angiogenesis by two-pronged: firstly, the extracellular domain of CD146 directly interacts with VEGFR-2, forms a complex with VEGFR-2 and VEGF which is a crucial step for VEGFR-2 activation. Secondly, the cytoplasmic tail of CD146 recruits ERMs and cytoskeleton, assembling the signalsome required for signal transduction from VEGFR-2 to AKT and p38 MAPKs.

In the SW1990 tumor model, we made use of bevacizumab, an anti-VEGF antibody as a combination partner for AA98. We believe that bevacizumab mediated its anti-tumor effect primarily through the blocking of

VEGF-VEGFR-2 signaling rather than VEGFR-1 although VEGF-A can bind both. This is because the two VEGF receptors differ in their binding affinities to VEGF-A and their function in angiogenesis. The binding of VEGF-A to VEGFR-2 on endothelial cells results in the phosphorylation of VEGFR-2 and angiogenesis. However, VEGF-A's interaction with VEGFR-1 acts as a negative regulator of angiogenesis due to the weaker phosphorylation of VEGFR-1, although the binding affinity of VEGF-A to VEGFR-1 is stronger than VEGFR-2.[39,40] In addition, our new data showing that CD146 does not interact with VEGFR-1 on endothelial cells (Figure. S7) suggests that the effect of bevacizumab on tumor angiogenesis occurs primarily through VEGFR-2 rather than VEGFR-1 although VEGF-A binds both VEGFR-2 and VEGFR-1.

Interestingly, AA98 and bevacizumab combination therapy showed additive effect on tumor angiogenesis in the SW1990 tumor model, which is in agreement with another study showing synergistic, pro-angiogenic effects between soluble CD146 and VEGF.[41] Therefore, the synergistic effect between the combined antibodies is due to the incomplete overlapping signaling of CD146 and VEGFR-2. In previous reports, we and others have found that CD146 can also function independently of VEGFR-2.[13,21,41] Additionally, VEGF can signal, at least in part, independently of CD146. For instance, the ERK pathway cannot be inhibited by anti-CD146 AA98 nor CD146-siRNA and other VEGF receptors such as VEGFR-1 can transduce VEGF signals. (Figure S7). This may help explain why anti-CD146 (AA98) in our combined therapy model does not completely inhibit angiogenesis.

AA98 targeting of CD146 in combination with bevacizumab could be exploited as a valid regimen in clinical therapy. Our finding provides a novel approach to inhibit tumor angiogenesis. Bevacizumab, a humanized monoclonal antibody targeting VEGF-A, is one of the most popular anti-angiogenesis drug and precedents exist for its use in combination with other agents in tumor therapy, including in colorectal cancer,[42] non-squamous-cell lung carcinoma (NSCLC),

metastatic renal cell carcinoma and glioblastoma multiforme.[43] However, the challenge of bevacizumab is its limited clinical application due to it effectiveness only on certain types of cancer.[44] For instance, bevacizumab is not very efficient for pancreatic cancer.[45] Thus, the dual targeting of CD146 and VEGF could prove more efficient for the treatment of pancreatic cancer and melanoma. This is the first report of the effectiveness of bevacizumab combinatorial therapy with a second antibody in the inhibition of tumors. In addition, bevacizumab was found to be effective only in metastatic colorectal cancer but not on stage 2 and 3 tumors,[46] suggesting that angiogenesis in the primary and metastatic tumor involve different mechanisms that require different treatments. CD146 has been implicated in the tumor progression of several cancers including colorectal cancer,[47] epithelial ovarian cancer,[48] and breast cancer.[18] Thus, bevacizumab in combination with anti-CD146 mAb AA98 may be a more effective treatment for metastatic tumors. However, this needs to be further investigated. In conclusion, this study provides evidence of a novel VEGFR-2 co-receptor and a promising strategy for combinatory anti-angiogenic therapy.

Acknowledgements

We thank Prof. Lena Claesson-Welsh for providing the human VEGFR-2 gene-containing pcDNA.3/ myc-His(+)B-VEGFR-2 plasmids and Dr. Irene Gramaglia for very carefully correction of the manuscript. This work was partly supported by grants from the National Basic Research Program of China (973 program) (2012CB934003, 2011CB915502, 2009CB521704, 2011CB933503), the National Important Science and Technology Specific projects (2012ZX10002-009, 2008ZX10004-005, 2009ZX09102-247), the National Natural Science Foundation of China (91029732, 20872173) and the Knowledge innovation Program of the Chinese Academy of Sciences (KSCX2-YW-M15).

Authorship

Tianxia Jiang designed, performed experiments, analyzed data and wrote the paper. Jie Zhuang and Yongting Luo assisted with the design of experiments, data analysis and image analysis. Hongxia Duan, Yongting Luo and Qiqun Zeng assisted with the animal experiments. Huiwen Yan assisted with experiments relating to signaling pathways. Kelong Fan constructed the C452A mutation of the CD146 gene. Zhongde Ye assisted with experiments relating to signaling pathways and reviewed the manuscript. Di Lu managed cell culture experiments. Junfeng Hao assisted with immunohistochemical analyses. Jing Feng and Dongling Yang assisted with data analysis. Xiyun Yan designed the project, designed experiments, analyzed the data, and reviewed the manuscript.

Conflict-of-interest disclosure: The authors declare no competing financial interest.

References

1. **Carmeliet, P., and Jain, R.K. Molecular mechanisms and clinical applications of angiogenesis. *Nature*. 2011;473(7347):298-307.**
2. **Grothey, A., and Galanis, E. Targeting angiogenesis: progress with anti-VEGF treatment with large molecules. *Nat Rev Clin Oncol*. 2009;6(9):507-518.**
3. **Tugues, S., Koch, S., Gualandi, L., et al. Vascular endothelial growth factors and receptors: anti-angiogenic therapy in the treatment of cancer. *Mol Aspects Med*. 2011;32(2):88-111.**
4. **Kaipainen, A., Korhonen, J., Mustonen, T., et al. Expression of the fms-like tyrosine kinase 4 gene becomes restricted to lymphatic endothelium during development. *Proc Natl Acad Sci U S A*. 1995;92(8):3566-3570.**
5. **Potente, M., Gerhardt, H., and Carmeliet, P. Basic and therapeutic aspects of angiogenesis. *Cell*. 2011;146(6):873-887.**
6. **Hurwitz, H., Fehrenbacher, L., Novotny, W., et al. Bevacizumab plus irinotecan, fluorouracil, and leucovorin for metastatic colorectal cancer. *N Engl J Med*. 2004;350(23):2335-2342.**
7. **Sandler, A., Gray, R., Perry, M.C., et al. Paclitaxel-carboplatin alone or with bevacizumab for non-small-cell lung cancer. *N Engl J Med*. 2006;355(24):2542-2550.**
8. **Yang, J.C., Haworth, L., Sherry, R.M., et al. A randomized trial of bevacizumab, an anti-vascular endothelial growth factor antibody, for metastatic renal cancer. *N Engl J Med*. 2003;349(5):427-434.**
9. **Miller, K., Wang, M., Gralow, J., et al. Paclitaxel plus bevacizumab versus paclitaxel alone for metastatic breast cancer. *N Engl J Med*. 2007;357(26):2666-2676.**
10. **Van Cutsem, E., Lambrechts, D., Prenen, H., et al. Lessons from the adjuvant bevacizumab trial on colon cancer: what next? *J Clin Oncol*. 2011;29(1):1-4.**
11. **Lehmann, J.M., Riethmuller, G., and Johnson, J.P. MUC18, a marker of tumor progression in human melanoma, shows sequence similarity to the neural cell adhesion molecules of the immunoglobulin superfamily. *Proc Natl Acad Sci U S A*. 1989;86(24):9891-9895.**
12. **Yan, X., Lin, Y., Yang, D., et al. A novel anti-CD146 monoclonal antibody, AA98, inhibits angiogenesis and tumor growth. *Blood*. 2003;102(1):184-191.**
13. **Kang, Y., Wang, F., Feng, J., et al. Knockdown of CD146 reduces the migration and proliferation of human endothelial cells. *Cell Res*. 2006;16(3):313-318.**
14. **So, J.H., Hong, S.K., Kim, H.T., et al. Gicerin/Cd146 is involved in zebrafish cardiovascular development and tumor angiogenesis. *Genes Cells*. 2010;15(11):1099-1110.**
15. **Bu, P., Gao, L., Zhuang, J., et al. Anti-CD146 monoclonal antibody AA98 inhibits angiogenesis via suppression of nuclear factor-kappaB activation. *Mol Cancer Ther*. 2006;5(11):2872-2878.**
16. **Liu, Q., Yan, X., Li, Y., et al. Pre-eclampsia is associated with the failure of melanoma**

cell adhesion molecule (MCAM/CD146) expression by intermediate trophoblast. *Lab Invest*. 2004;84(2):221-228.

17. **Liu, Q., Zhang, B., Zhao, X., et al. Blockade of adhesion molecule CD146 causes pregnancy failure in mice. *J Cell Physiol*. 2008;215(3):621-626.**
18. **Zeng, Q., Li, W., Lu, D., et al. CD146, an epithelial-mesenchymal transition inducer, is associated with triple-negative breast cancer. *Proc Natl Acad Sci U S A*. 2012;109(4):1127-1132.**
19. **Ouhtit, A., Gaur, R.L., Abd Elmageed, Z.Y., et al. Towards understanding the mode of action of the multifaceted cell adhesion receptor CD146. *Biochim Biophys Acta*. 2009;1795(2):130-136.**
20. **Bu, P., Zhuang, J., Feng, J., et al. Visualization of CD146 dimerization and its regulation in living cells. *Biochim Biophys Acta*. 2007;1773(4):513-520.**
21. **Zheng, C., Qiu, Y., Zeng, Q., et al. Endothelial CD146 is required for in vitro tumor-induced angiogenesis: the role of a disulfide bond in signaling and dimerization. *Int J Biochem Cell Biol*. 2009;41(11):2163-2172.**
22. **Anfosso, F., Bardin, N., Frances, V., et al. Activation of human endothelial cells via S-endo-1 antigen (CD146) stimulates the tyrosine phosphorylation of focal adhesion kinase p125(FAK). *J Biol Chem*. 1998;273(41):26852-26856.**
23. **Anfosso, F., Bardin, N., Vivier, E., et al. Outside-in signaling pathway linked to CD146 engagement in human endothelial cells. *J Biol Chem*. 2001;276(2):1564-1569.**
24. **Zhang, Y., Zheng, C., Zhang, J., et al. Generation and characterization of a panel of monoclonal antibodies against distinct epitopes of human CD146. *Hybridoma (Larchmt)*. 2008;27(5):345-352.**
25. **Luo, Y., Zheng, C., Zhang, J., et al. Recognition of CD146 as an ERM-binding protein offers novel mechanisms for melanoma cell migration. *Oncogene*. 2012;31(3):306-321.**
26. **Nagata, D., Mogi, M., and Walsh, K. AMP-activated protein kinase (AMPK) signaling in endothelial cells is essential for angiogenesis in response to hypoxic stress. *J Biol Chem*. 2003;278(33):31000-31006.**
27. **Redmond, E.M., Cullen, J.P., Cahill, P.A., et al. Endothelial cells inhibit flow-induced smooth muscle cell migration: role of plasminogen activator inhibitor-1. *Circulation*. 2001;103(4):597-603.**
28. **Tremmel, M., Matzke, A., Albrecht, I., et al. A CD44v6 peptide reveals a role of CD44 in VEGFR-2 signaling and angiogenesis. *Blood*. 2009;114(25):5236-5244.**
29. **Yancopoulos, G.D. Clinical application of therapies targeting VEGF. *Cell*. 2010;143(1):13-16.**
30. **Bevacizumab. Anti-VEGF monoclonal antibody, avastin, rhumab-VEGF. *Drugs R D*. 2002;3(1):28-30.**
31. **Orian-Rousseau, V., Chen, L., Sleeman, J.P., et al. CD44 is required for two consecutive steps in HGF/c-Met signaling. *Genes Dev*. 2002;16(23):3074-3086.**
32. **Palyi-Krekk, Z., Barok, M., Kovacs, T., et al. EGFR and ErbB2 are functionally coupled to CD44 and regulate shedding, internalization and motogenic effect of CD44. *Cancer Lett*. 2008;263(2):231-242.**
33. **Meran, S., Luo, D.D., Simpson, R., et al. Hyaluronan facilitates transforming growth factor-beta1-dependent proliferation via CD44 and epidermal growth factor receptor**

interaction. *J Biol Chem*. 2011;286(20):17618-17630.

34. **Olaku, V., Matzke, A., Mitchell, C., et al. c-Met recruits ICAM-1 as a coreceptor to compensate for the loss of CD44 in Cd44 null mice. *Mol Biol Cell*. 2011;22(15):2777-2786.**
35. **Francavilla, C., Loeffler, S., Piccini, D., et al. Neural cell adhesion molecule regulates the cellular response to fibroblast growth factor. *J Cell Sci*. 2007;120(Pt 24):4388-4394.**
36. **Whitaker, G.B., Limberg, B.J., and Rosenbaum, J.S. Vascular endothelial growth factor receptor-2 and neuropilin-1 form a receptor complex that is responsible for the differential signaling potency of VEGF(165) and VEGF(121). *J Biol Chem*. 2001;276(27):25520-25531.**
37. **Favier, B., Alam, A., Barron, P., et al. Neuropilin-2 interacts with VEGFR-2 and VEGFR-3 and promotes human endothelial cell survival and migration. *Blood*. 2006;108(4):1243-1250.**
38. **Voltz, J.W., Brush, M., Sikes, S., et al. Phosphorylation of PDZ1 domain attenuates NHERF-1 binding to cellular targets. *J Biol Chem*. 2007;282(46):33879-33887.**
39. **Sawano, A., Iwai, S., Sakurai, Y., et al. Flt-1, vascular endothelial growth factor receptor 1, is a novel cell surface marker for the lineage of monocyte-macrophages in humans. *Blood*. 2001;97(3):785-791.**
40. **Waltenberger, J., Claesson-Welsh, L., Siegbahn, A., et al. Different signal transduction properties of KDR and Flt1, two receptors for vascular endothelial growth factor. *J Biol Chem*. 1994;269(43):26988-26995.**
41. **Harhouri, K., Kebir, A., Guillet, B., et al. Soluble CD146 displays angiogenic properties and promotes neovascularization in experimental hind-limb ischemia. *Blood*. 2010;115(18):3843-3851.**
42. **Escudier, B., Pluzanska, A., Koralewski, P., et al. Bevacizumab plus interferon alfa-2a for treatment of metastatic renal cell carcinoma: a randomised, double-blind phase III trial. *Lancet*. 2007;370(9605):2103-2111.**
43. **Friedman, H.S., Prados, M.D., Wen, P.Y., et al. Bevacizumab alone and in combination with irinotecan in recurrent glioblastoma. *J Clin Oncol*. 2009;27(28):4733-4740.**
44. **Van Meter, M.E., and Kim, E.S. Bevacizumab: current updates in treatment. *Curr Opin Oncol*. 2010;22(6):586-591.**
45. **Van Cutsem, E., Vervenne, W.L., Bennouna, J., et al. Phase III trial of bevacizumab in combination with gemcitabine and erlotinib in patients with metastatic pancreatic cancer. *J Clin Oncol*. 2009;27(13):2231-2237.**
46. **Allegra, C.J., Yothers, G., O'Connell, M.J., et al. Phase III trial assessing bevacizumab in stages II and III carcinoma of the colon: results of NSABP protocol C-08. *J Clin Oncol*. 2011;29(1):11-16.**
47. **Adachi, K., Hattori, M., Kato, H., et al. Involvement of gicerin, a cell adhesion molecule, in the portal metastasis of rat colorectal adenocarcinoma cells. *Oncol Rep*. 2010;24(6):1427-1431.**
48. **Aldovini, D., Demichelis, F., Doglioni, C., et al. M-CAM expression as marker of poor prognosis in epithelial ovarian cancer. *Int J Cancer*. 2006;119(8):1920-1926.**

Figure legends

Figure 1. CD146 interacts directly with VEGFR-2.

A: Co-immunoprecipitation (Co-IP) assays showed that endogenous CD146 associates with VEGFR-2 in HUVEC. CD146 and VEGFR-2 from cell lysates were immunoprecipitated with anti-CD146 mAb AA1 and anti-VEGFR-2, respectively. Western blotting was performed using anti-VEGFR-2 antibody and mAb AA1.

B: Co-IP assays showed the association of CD146 and VEGFR-2 in CD146-expressing HEK293T cells. Cells were transiently transfected with the VEGFR-2-expressing construct or empty vectors. Proteins were precipitated by anti-VEGFR-2 antibody, and examined by immunoblot using antibodies against CD146.

C: Direct interaction between the sCD146 and sVEGFR-2 *in vitro*. Fc-VEGFR2 was first bound to protein G-beads which were then incubated with His-sCD146. Bound proteins were subsequently analyzed by Western blotting. The interaction between VEGF and Fc-VEGFR-2 served as a positive control and Fc served as a negative control.

D: The interaction between CD146 and VEGFR-2 in HUVECs is blocked by anti-CD146 AA98 but not by AA1. HUVECs were first treated with anti-CD146, AA98 or AA1, prior to immunoprecipition with VEGFR-2 antibody and Western blotting with CD146 antibody. Cell lysates were blotted with anti-CD146 mAb AA1.

E: Mutant CD146/C452A impaired the interaction between CD146 and VEGFR-2. HUVECs transfected with CD146/C452A or an empty vector were immunoprecipitated with anti-VEGFR-2 and then immunoblotted with anti-VEGFR-2 or AA1. Cell lysates were blotted with anti-his antibody targeting CD146/C452A-His.

Figure 2. The anti-CD146 mAb AA98 blocks VEGF-induced VEGFR-2 phosphorylation, Akt/p38/NF-κB activation.

A: Phosphorylation of VEGFR-2 induced by VEGF in HUVECs was assessed in the presence

of anti-CD146 mAbs AA98 or AA1. Total VEGFR-2quantification was determined by measuring the band density and then normalizing against internal controls,. Results are presented as the means ± SEM of normalized values from three independent assays.

B: P38 activation induced by VEGF in the presence of AA98 or AA1 was assessed.

C-D: NF-κB (p-p65 and IκBα) activation by VEGF in the presence of AA98 or AA1 as indicated.

E: Akt activation induced by VEGF in the presence of AA98 or AA1 was measured.

F: Immunofluorescence showing inhibition of AA98 on the translocation of p65 and p50 from the cytoplasm to nucleus, NF-κB activation was detected using specific anti-p65 and anti-p50 antibodies (scale bar, 20 μm). *P<.05, ** P<.01.

Figure 3. CD146 is required for VEGF-mediated signal transduction.

A: Phosphorylation of VEGFR-2 induced by VEGF was determined after HUVECs were co-transfected with CD146-siRNA and pcDNA3.1-CD146. The quantification of the relative p-VEGFR-2/VEGFR-2 index is shown. At least three independent assays were performed.

B: AKT activation induced by VEGF was measured after HUVECs were co-transfected with CD146-siRNA and pcDNA3.1-CD146.

C: P38 activation under treatment as indicated was measured.

D: NF-κB activation induced by VEGF after rescuing CD146 expression was measured. Western blots were quantified by measuring band density which was then normalized to GAPDH. Bar graphs (means ± SEM) present normalized values from at least three independent experiments.

E: Immunofluorescence showing the role of CD146 in NF-κB nuclear translocation. NF-κB was detected using specific anti-p65 and anti-p50 antibodies (scale bar, 20 μm). *P<.05, ** P<.01, *** P<.001, NS.: not significant.

Figure 4. VEGFR-2 signaling is dependent on CD146 binding to Moesin.

A: A CD146 construct lacking the conserved positively-charged amino-acid KKGK motif

(CD146-△KKGK) was transiently transfected into HUVECs. Activation of VEGFR-2 induced by VEGF and signaling to AKT and p38 were determined.

B: Moesin lacking the actin-binding domain (Moesin-△ABD) was transiently transfected into HUVECs. Activation of VEGFR-2 on induction with VEGF and signaling to AKT or p38 were determined.

C-D: The migrated capability of HUVECs induced by VEGF was determined after transfected with CD146-△KKGK or Moesin-△ABD. Cell migration was determined using a transwell system as described in "Cell migration assay". Data were collected from three wells. Representative images of migrated cells were also shown. *P<.05, ** P<.01, NS.: not significant.

Figure 5. CD146 is required in VEGF-induced cell migration and tube formation

A: Cell migration was determined using a transwell system. HUVECs were induced by VEGF in the presence of anti-CD146 mAbs AA98 or AA1 as indicated. The number of migrating cells was counted. Data were collected from three wells. Representative images of migrated cells were also shown.

B: VEGF-induced tube formation was quantified in the presence of anti-CD146 mAb AA98 or AA1 by counting the total vessel length per field. Data were collected from three wells.

C: Cells co-transfected with CD146-siRNA and pcDNA3.1-CD146 were subjected to "Cell migration assays" as described. The number of cells migrating through the filters was recorded. The number of cells per optic field is presented as the mean ± SEM of at least three independent assays.

D: Cells co-transfected with CD146-siRNA and pcDNA3.1-CD146 were subjected to "Tube formation assays" as described. Results presented are total tube lengths from three independent tests (means ± SEM). *P<.05, ** P<.01, *** P<.001, NS.: not significant.

Figure 6. VEGF-induced vascularization is impaired in CD146$^{EC\text{-}KO}$ mice

A: Immunofluorescence showing the vascularization induced by VEGF in the Matrigel explanted in WT and CD146$^{EC\text{-}KO}$ mice. Staining of blood vessels was performed with a CD31

antibody (red); green indicates CD146 (Rat anti-CD146, ME-9F1) staining. Nuclei were stained with DAPI (blue). Ten mice were included in each group. Bar represents 50 μm**.**

B: The graph represents average vessel number in five random fields of each section. *** *P*<.001.

Figure 7. The combination of anti-CD146 AA98 and anti-VEGF bevacizumab has cumulative antitumor effects on human parcreatic carcinoma growth and angiogenesis *in vivo*

A: Representation of human pancreatic carcinoma in xenografted mice following the administration indicated.

B: Mean tumor volumes at specific time points after injection of human pancreatic carcinoma cells SW1990 (n=10) under the treatments indicated.

C: When tumor size reached approximately 3 cm^3, mice were sacrificed, and tumors were excised and weighed. Tumor weight was determined and evaluated in the graphs.

D: Microvascular density of tumors under indicated administration. Sections from human pancreatic carcinoma under indicated treatments were stained with anti-CD31antibody (scale bar, 100 μm). Statistical significance was calculated with the unpaired Student's t test. **P*<.05, ** *P*<.01, *** *P*<.001.

Figure 1

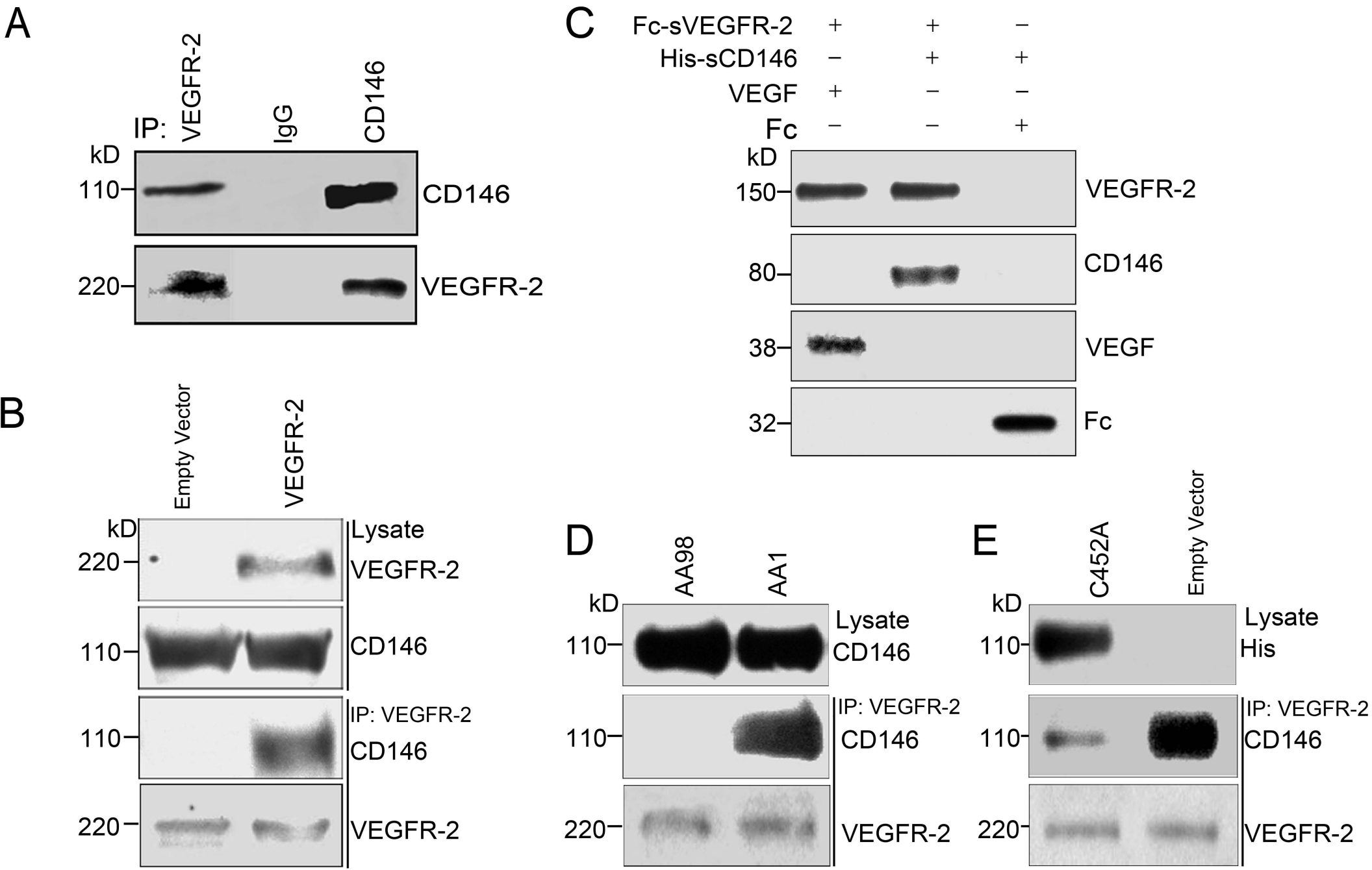
A
IP: VEGFR-2
IgG
CD146
kD
110
CD146
220
VEGFR-2
B
Empty Vector
VEGFR-2
kD
220
Lysate
VEGFR-2
110
CD146
110
IP: VEGFR-2
CD146
220
VEGFR-2
C
Fc-sVEGFR-2 + + −
His-sCD146 − + +
VEGF + − −
Fc − − +
kD
150
VEGFR-2
80
CD146
38
VEGF
32
Fc
D
AA98
AA1
kD
110
Lysate
CD146
110
IP: VEGFR-2
CD146
220
VEGFR-2
E
C452A
Empty Vector
kD
110
Lysate
His
110
IP: VEGFR-2
CD146
220
VEGFR-2

Figure 2

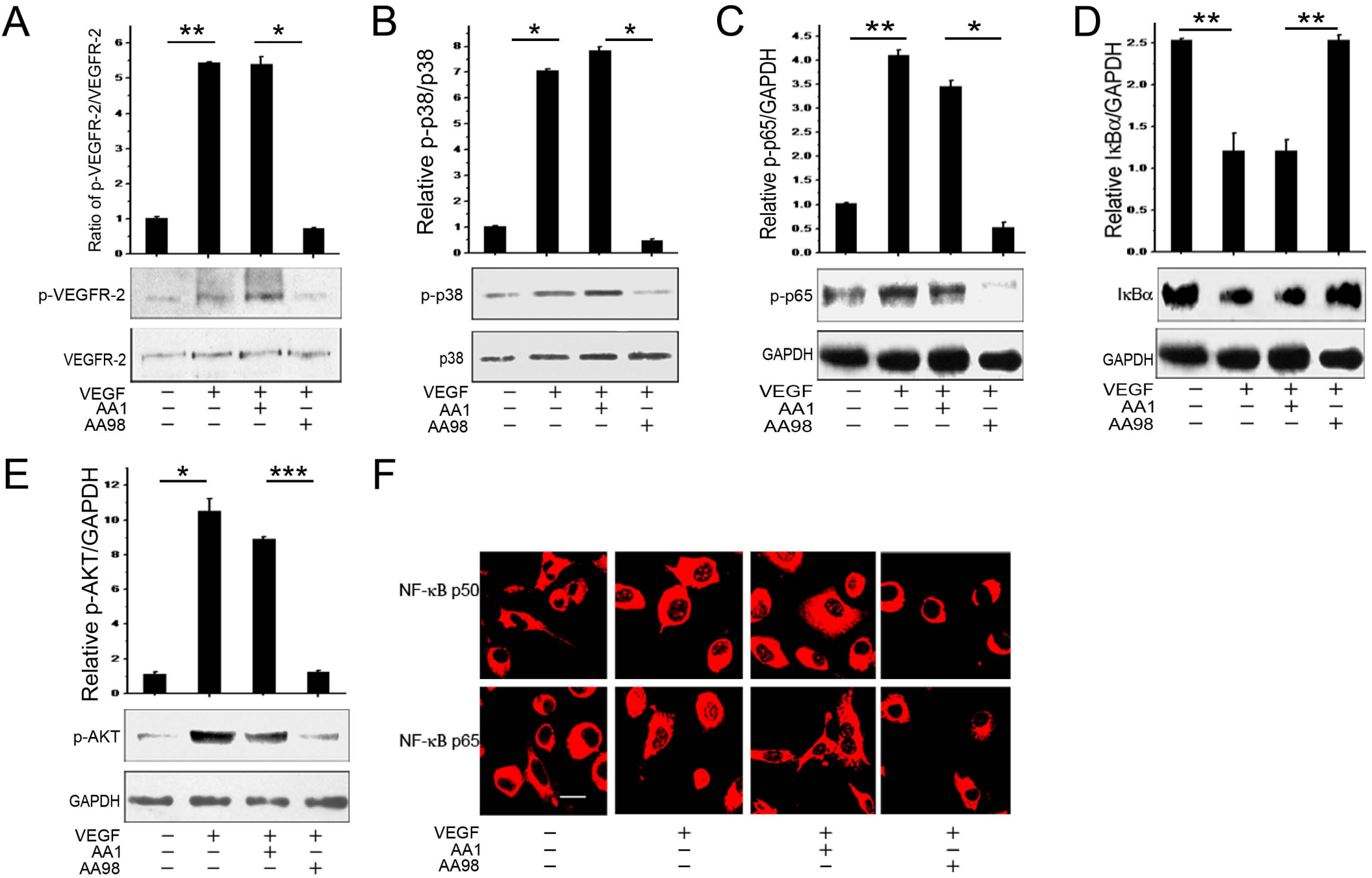
A
Ratio of p-VEGFR-2/VEGFR-2
**
*
p-VEGFR-2
VEGFR-2
VEGF – + + +
AA1 – – + –
AA98 – – – +
B
Relative p-p38/p38
*
*
p-p38
p38
VEGF – + + +
AA1 – – + –
AA98 – – – +
C
Relative p-p65/GAPDH
**
*
p-p65
GAPDH
VEGF – + + +
AA1 – – + –
AA98 – – – +
D
Relative IκBα/GAPDH
**
**
IκBα
GAPDH
VEGF – + + +
AA1 – – + –
AA98 – – – +
E
Relative p-AKT/GAPDH
*
***
p-AKT
GAPDH
VEGF – + + +
AA1 – – + –
AA98 – – – +
F
NF-κB p50
NF-κB p65
VEGF – + + +
AA1 – – + –
AA98 – – – +

Figure 3

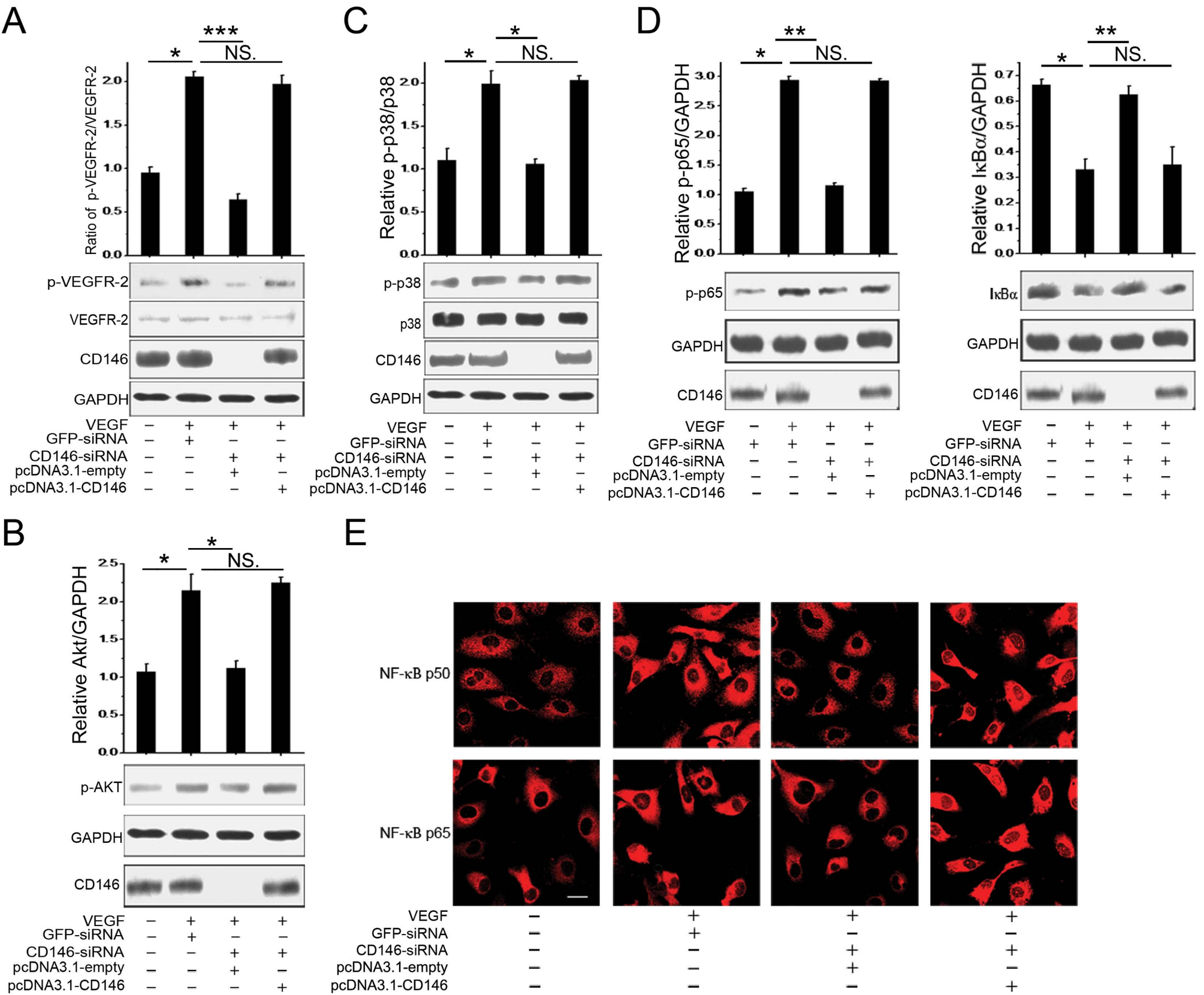
A
Ratio of p-VEGFR-2/VEGFR-2
p-VEGFR-2
VEGFR-2
CD146
GAPDH
VEGF
GFP-siRNA
CD146-siRNA
pcDNA3.1-empty
pcDNA3.1-CD146
B
Relative Akt/GAPDH
p-AKT
GAPDH
CD146
C
Relative p-p38/p38
p-p38
p38
CD146
GAPDH
D
Relative p-p65/GAPDH
p-p65
GAPDH
CD146
Relative IκBα/GAPDH
IκBα
GAPDH
CD146
E
NF-κB p50
NF-κB p65
NS.

Figure 4

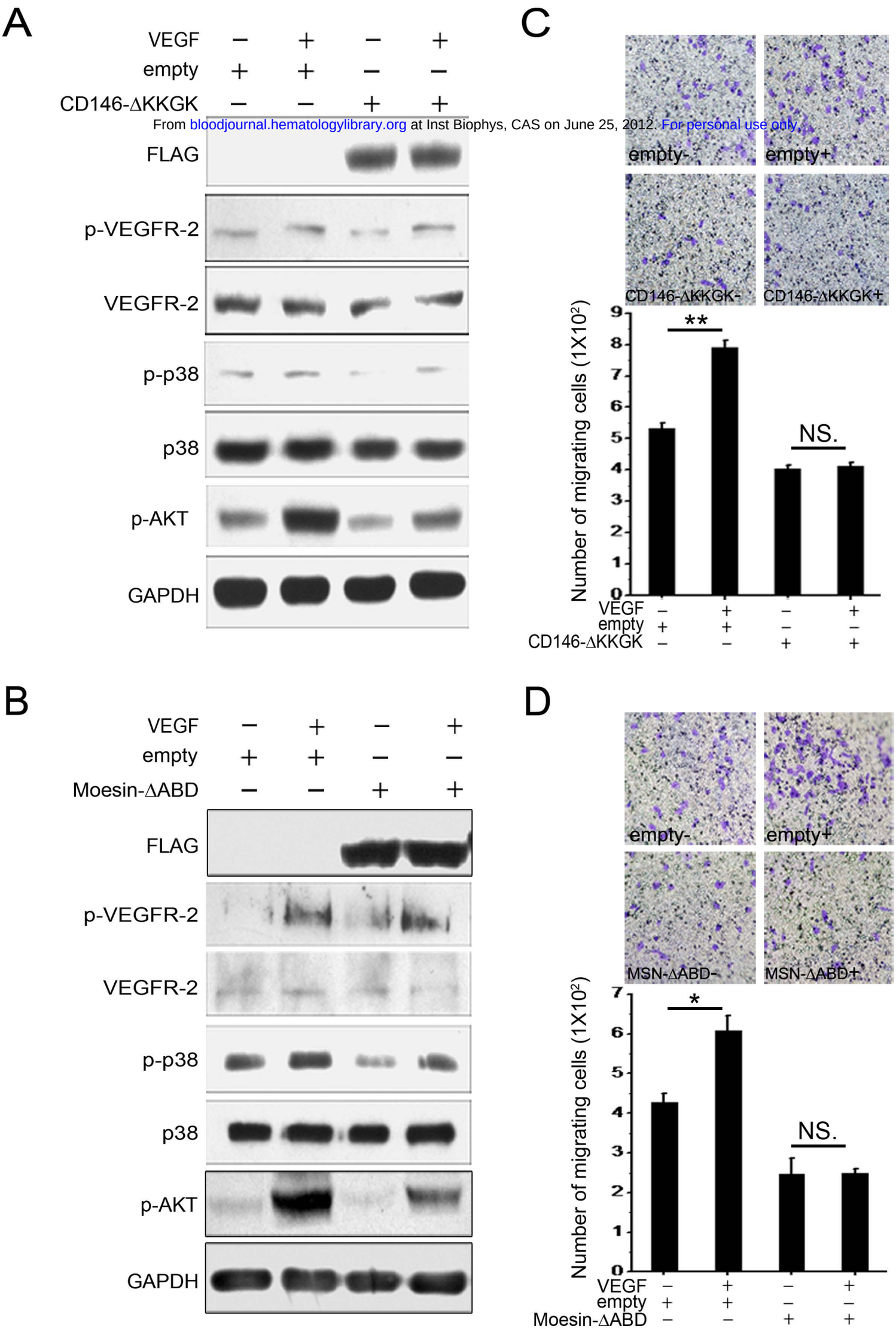

Figure 5

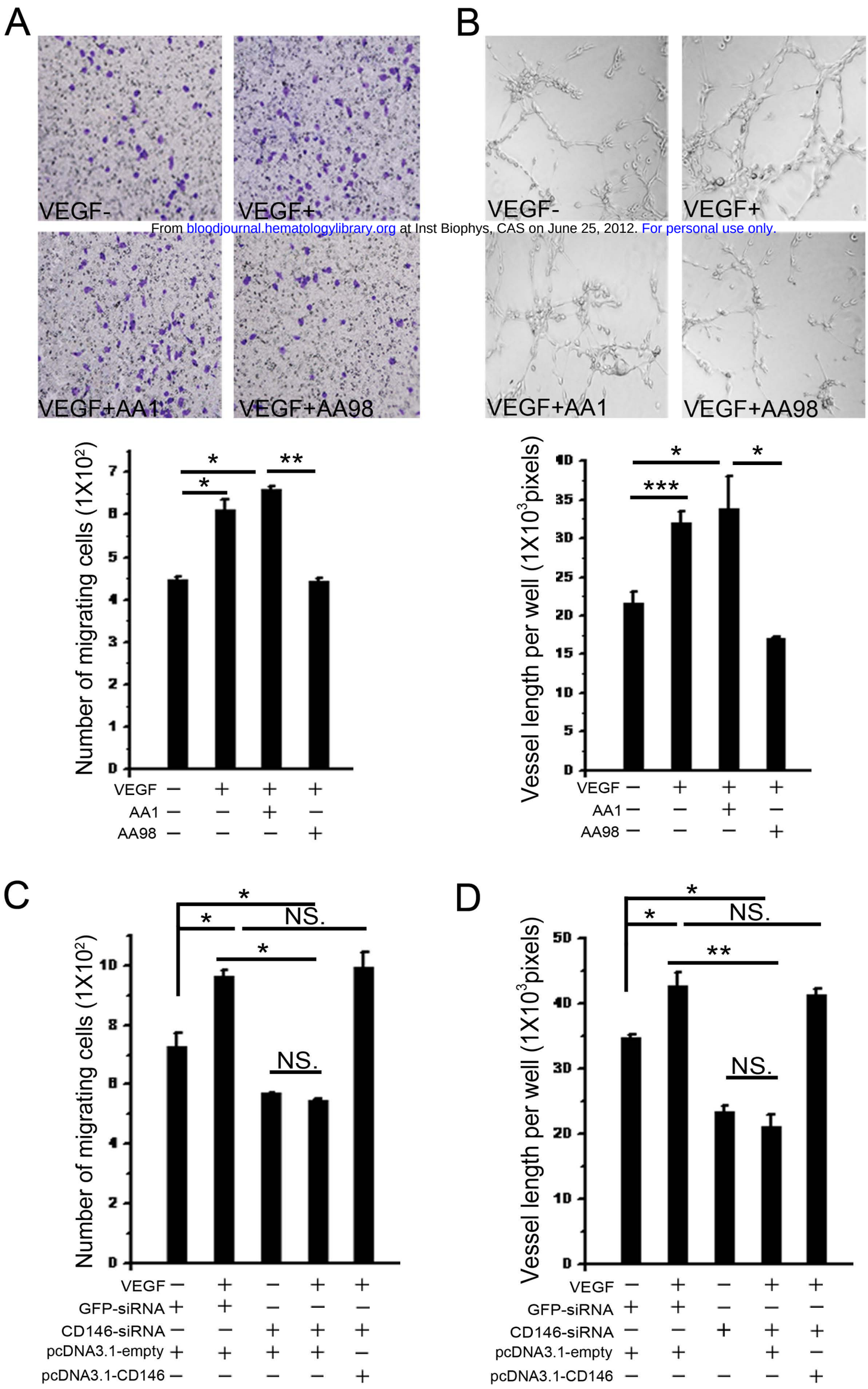

Figure 6

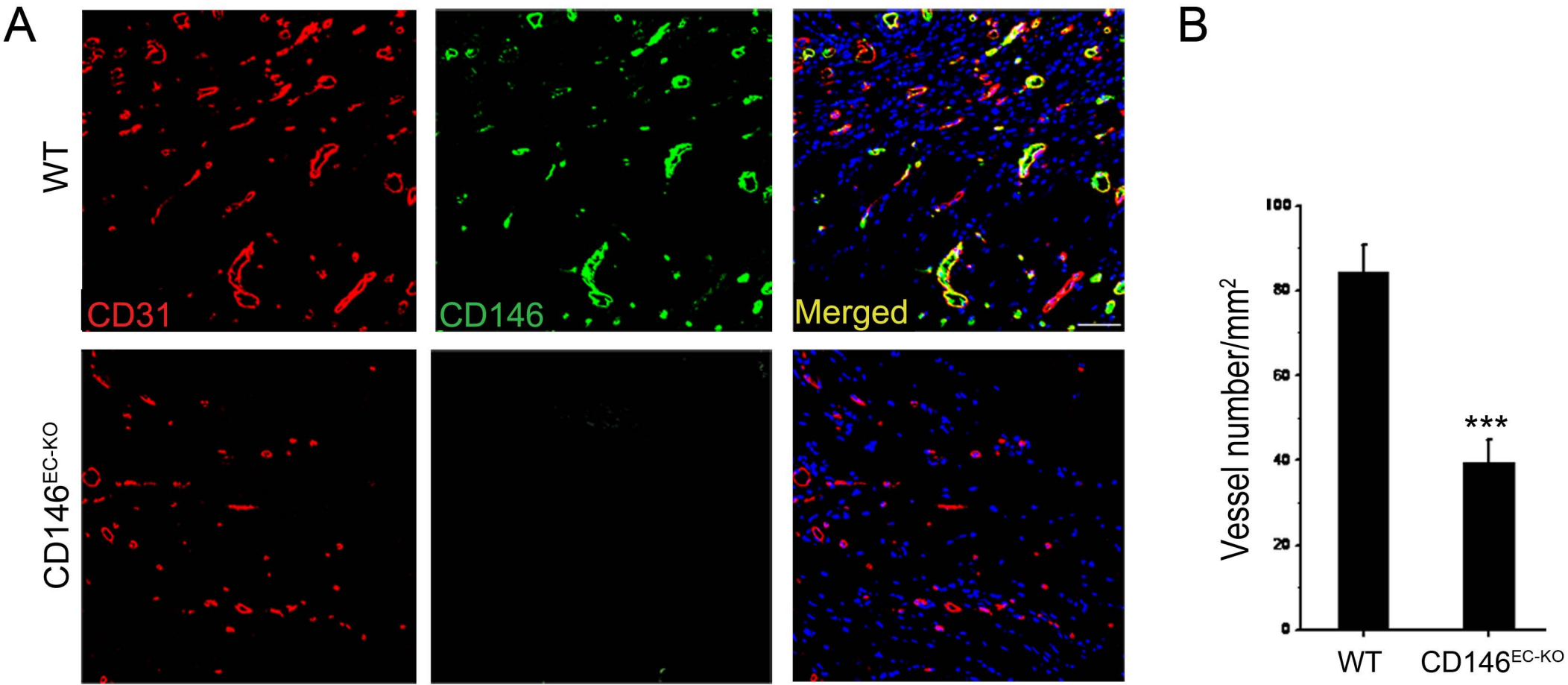
A
WT
CD146EC-KO
CD31
CD146
Merged
B
Vessel number/mm2
100
80
60
40
20
0
***
WT
CD146EC-KO

Figure 7

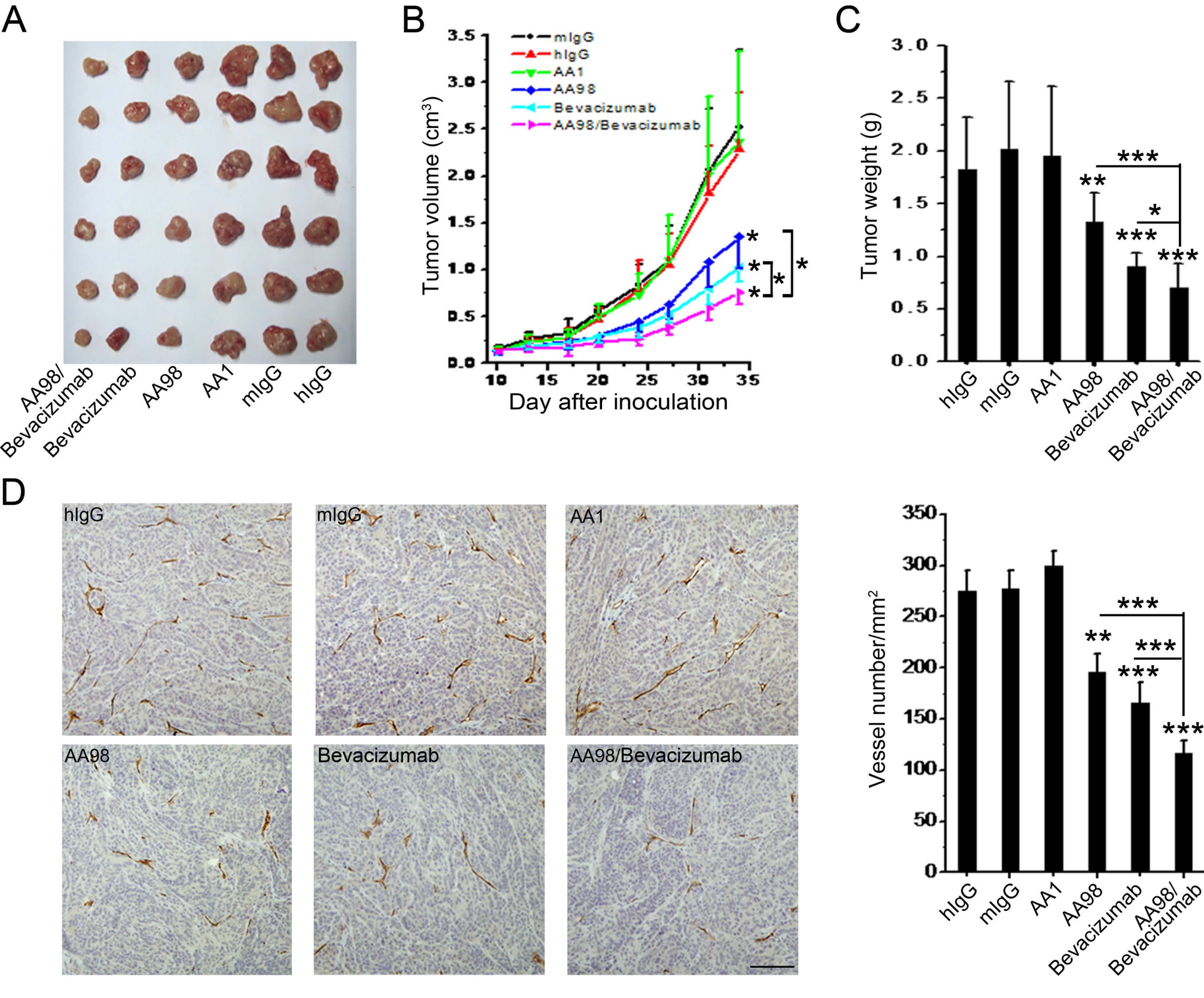
A
AA98/ Bevacizumab
Bevacizumab
AA98
AA1
mIgG
hIgG
B
mIgG
hIgG
AA1
AA98
Bevacizumab
AA98/Bevacizumab
Tumor volume (cm³)
Day after inoculation
C
Tumor weight (g)
hIgG
mIgG
AA1
AA98
Bevacizumab
AA98/ Bevacizumab
D
hIgG
mIgG
AA1
AA98
Bevacizumab
AA98/Bevacizumab
Vessel number/mm²